Structure of cytochrome *c′*: a dimeric, high-spin haem protein

Patricia C. Weber*§, R. G. Bartsch†, M. A. Cusanovich*, R. C. Hamlin‡, A. Howard‡, S. R. Jordan*, M. D. Kamen†, T. E. Meyer†, D. W. Weatherford*, Nguyen huu Xuong‡ & F. R. Salemme*

*Departments of Biochemistry and Chemistry, New Chemistry Building, University of Arizona, Tucson, Arizona 85721
†Department of Chemistry A-002, University of California at San Diego, La Jolla, California 92093
‡Departments of Physics, Chemistry and Biology, University of California at San Diego, La Jolla, California 92093
§To whom correspondence should be addressed

The bacterial cytochromes *c′* (ref. 1) occur in various photosynthetic and denitrifying bacteria, where they are presumed to function in electron transport[2]. Most cytochromes *c′* are isolated as dimeric molecules composed of two identical subunits of ~14,000 molecular weight (MW), with each polypeptide chain incorporating a protohaem IX prosthetic group covalently bound through thioether linkages formed by condensation of two cysteine side chains with the haem vinyl groups[3]. Although a similar mode of covalent haem attachment is found in members of the well studied mitochondrial cytochrome *c* family[4], the cytochromes *c′* are, in contrast, high-spin haem proteins (hence the prime designation) which bind neutral ligands[5], characteristic properties generally associated with members of the oxygen-binding globin family[6]. Here we present a preliminary structural description of the cytochrome *c′* derived from the photosynthetic, purple non-sulphur bacterium *Rhodospirillum molischianum*, and show that it bears little structural resemblance to members of either the cytochrome *c* or globin structural families. The cytochrome *c′* monomer structure is, instead, principally organized as a left-twisted, 4-α-helical bundle, a structural motif previously observed in several other sequentially and functionally unrelated proteins[7–13].

R. molischianum cytochrome *c′* crystallizes in the orthorhombic space group $P2_12_12_1$ ($a=56.5$ Å, $b=71.8$ Å, $c=75.6$ Å) with a dimeric molecule (MW ~ 29,000) in the crystallographic asymmetric unit[14]. Native and heavy atom (K_2PtCl_6 and K_2HgI_4) intensity data were collected from three crystals on the multiwire area detector developed by Xuong and co-workers at the University of California at San Diego[15,16]. Heavy atom sites for the singly substituted platinum and doubly substituted mercury derivatives were determined by deconvolution of the respective heavy atom difference Patterson maps and referred to a common origin by calculating a difference Fourier map for each derivative based on phases derived from the other. Anomalous dispersion effects arising from the platinum and mercury derivatives were incorporated into the final phase refinement cycles (Table 1) as described by Matthews[17], giving an overall figure of merit of 0.72 for the 10,667 independent reflections phased to 2.5 Å resolution. The resulting map was contoured to allow construction of a 2 cm Å^{-1} Kendrew model of the dimer, which was built according to the established amino acid sequence of the molecule[18]. Preliminary atomic coordinates were measured from the model using an electro-mechanical optical superpositioning device[19]. Figure 1 shows a representative view of the electron density of the 2.5 Å resolution map, whose overall quality was sufficient to trace unambiguously the backbone chain and establish the majority of the side-chain conformations.

Table 1 Data collection and phase refinement for *R. molischianum* cytochrome *c′*

Crystal	Native	K_2PtCl_6*	K_2HgI_4†
No. of intensities measured (observations/unique reflections)	81,380/18,513	71,072/10,881	67,994/14,082
Scaling *R*	0.062	0.074	0.068
No. of reflections used in phase refinement	10,667	10,372	10,540
R_C	—	0.55	0.54
R_K	—	0.084	0.095
E/F_H	—	0.37	0.48
E''/E	—	0.23	0.25

The overall figure of merit, *m*, to 2.5 Å resolution is 0.72. *E*, *E″* = r.m.s. differences between observed and calculated heavy atom and anomalous dispersion contributions, respectively. F_H = mean heavy atom contribution.

*Platinum site at $x/a=0.402$, $y/b=0.236$, $z/c=0.144$, $B=16.6$ Å^2.

†Mercury site 1 at $x/a=0.082$, $y/b=0.073$, $z/c=0.061$, $B=32.0$ Å^2, and mercury site 2 at $x/a=0.253$, $y/b=0.321$, $z/c=0.386$, $B=40.1$ Å^2.

$$R_C=\frac{\Sigma\left||F_{PH}\pm F_P|-F_H(\text{calc})\right|}{\Sigma|F_{PH}\pm F_P|}\quad\text{for centric reflections.}$$

$$R_K=\frac{\Sigma|F_{PH}(\text{obs})-F_{PH}(\text{calc})|}{F_{PH}(\text{obs})}$$

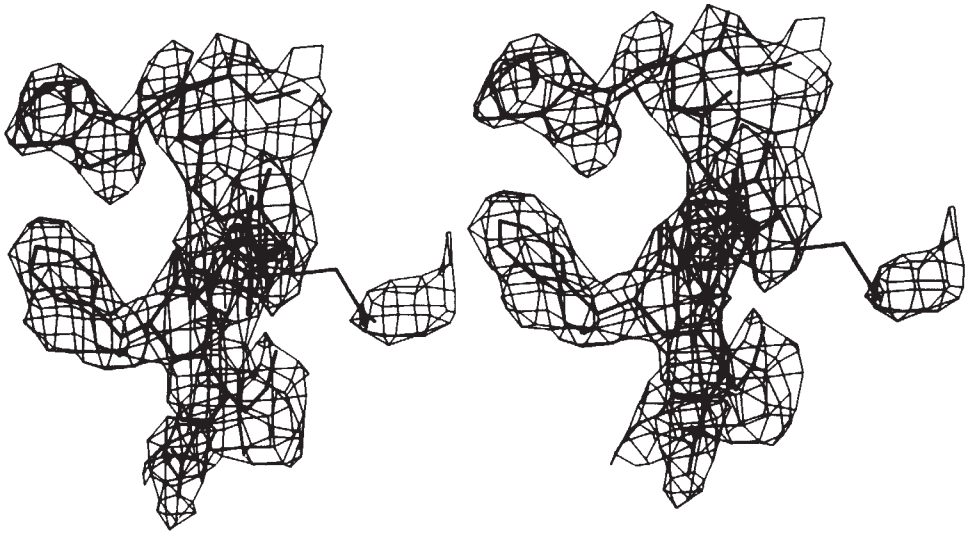

Fig. 1 Steroscopic view of a segment of the C helix (residues Glu 81, Phe, Leu, Glu, Gly, Trp 86) superimposed on the 2.5 Å resolution MIR phased electron density map, showing a representative fit of the measured model coordinates. Prominent in the density are two aromatic residues situated in the protein interior and an external, solvent-exposed glutamate whose side chain is only partially defined at the present contour level which includes 15% of the unit cell volume.

0028-0836/80/290302-03$01.00

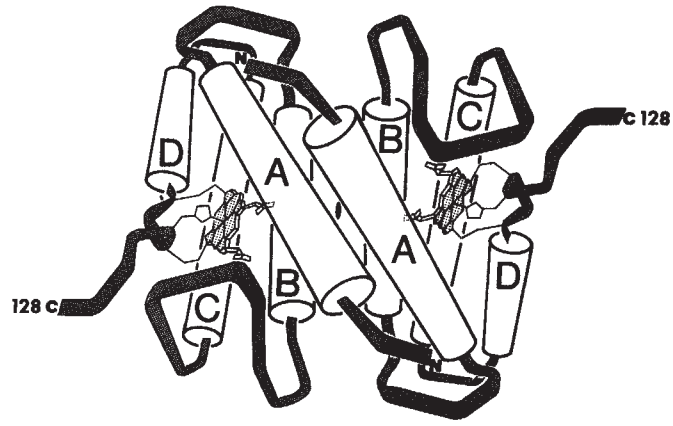

Fig. 2 Schematic representation of the *R. molischianum* cytochrome *c'* dimer viewed down the molecular diad axis. The cytochrome *c'* monomers are principally composed of four, roughly parallel α-helices shown here as sequentially labelled cylinders. The left-twisted 4-α-helical arrangement of the monomers is qualitatively repeated at the subunit interface, due to the pairwise interaction of two helices from each subunit. The haem groups, situated at one end of the helical bundle, are orientated roughly parallel to each other and to the subunit interface, with their propionate side chains pointed towards the molecular surface. Regions of essentially extended polypeptide chain (shaded) connect and terminate the helices in each monomer. Approximately one-half of the residues in the molecule exist in an α-helical conformation.

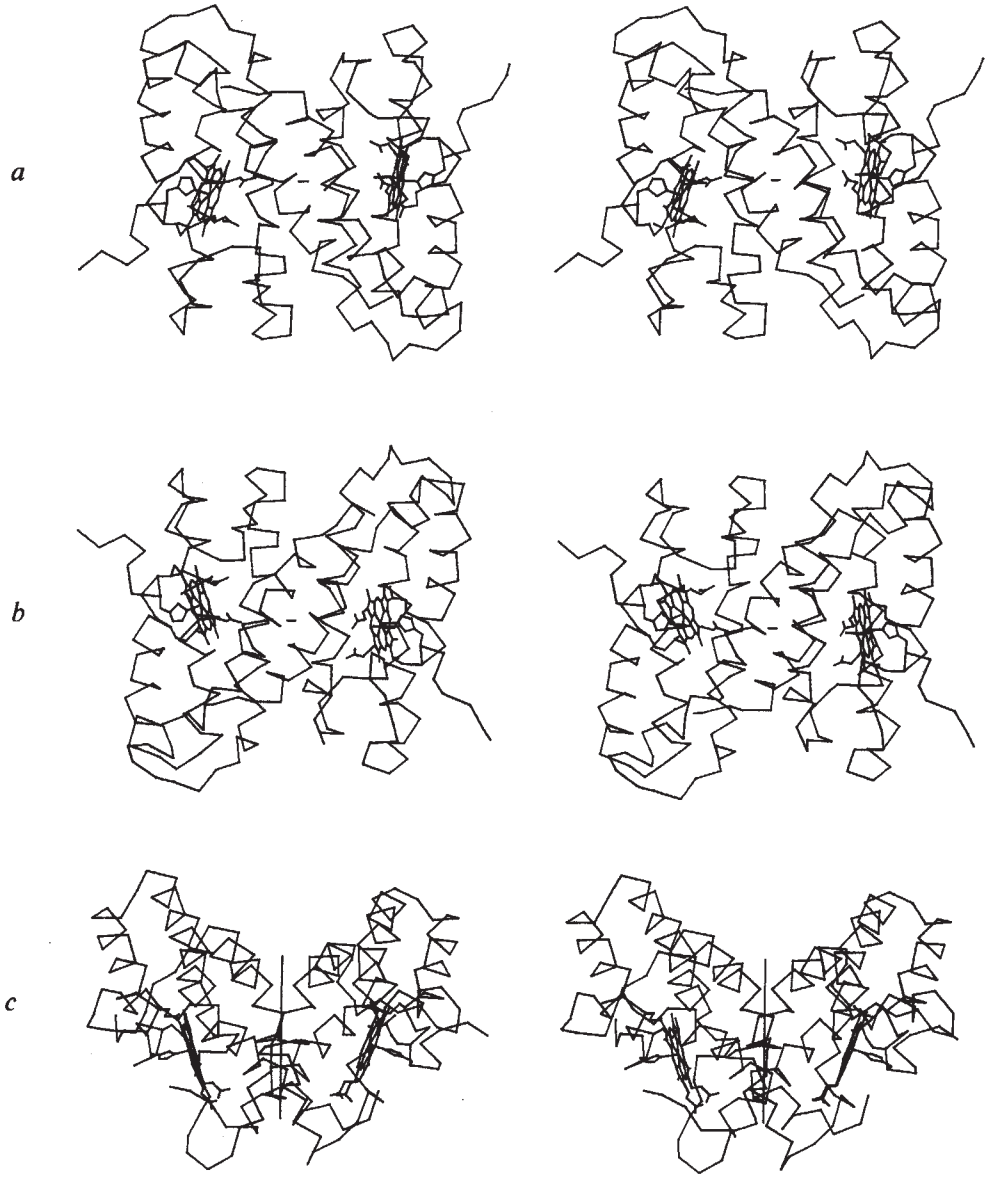

Fig. 3 Stereoscopic α-carbon drawings of *R. molischianum* cytochrome *c'*. *a* Shows the structure from the same aspect as Fig. 2, looking down the molecular diad axis at the molecular surface which has greatest haem exposure. The haem prosthetic groups, covalently bound near the carboxy termini, are separated in space by the two A helices, one from each subunit, which form the closest inter-helical interaction in the entire structure. The regions of extended polypeptide between helices are orientated towards this 'haem side' of the dimer. In contrast, the opposite side shown in *b* is primarily composed of α-helices. The ~110° crossing angle between subunits gives the dimer a V-shaded appearance when viewed normal to the diad axis as in *c*.

Figures 2 and 3 show schematic and α-carbon stereo representations of the cytochrome *c'* dimer. Each subunit is composed of a 128-amino acid polypeptide chain incorporating a covalently bound protohaem IX prosthetic group. Structurally, each monomer is composed of four, roughly parallel α-helices (sequentially labelled A–D) connected by more or less extended loops which join adjacent helix ends. Additional regions of essentially extended polypeptide chain occur at both the amino and carboxy termini of the molecule, the latter providing the covalent attachment points for the haem prosthetic group. The α-helices of the monomer pack with an overall left-handed twist along the direction of the helix axes. However, the helices of the bundle distinctly diverge at one end to accommodate the haem prosthetic group.

The cytochrome *c'* monomers pack about a non-crystallographic diad axis at an angle between bundle axes of approximately 110°, giving the dimer a V-shaped appearance when viewed normal to the diad symmetry axis (Fig. 3*c*). The subunit interaction is mediated by the pairwise interaction of the A and B helices of each monomer, to give a 4-α-helical, left-twisted AA′–BB′ bundle at the dimer interface whose

geometry is qualitatively similar to the arrangement of the helices within each monomer. The fact that the subunit interface interactions are similar to those within each monomer, both with respect to the hydrophobic nature of the amino acid residues involved and the overall similarity in extent and geometry of the α-helical interactions, provides an explanation for the observation that some homologous species of cytochrome *c′* can only be dissociated in conditions which lead to protein denaturation[20].

The protohaem IX prosthetic group in cytochrome *c′* forms three covalent attachments with the polypeptide chain, all of which are derived from the pentapeptide sequence Cys-X-X-Cys-His at residues 118–122. Two of these are the haem thioether linkages which serve to orientate the haem so that its propionate-substituted edge lies roughly parallel to each monomer bundle axis, and roughly perpendicular to the dimer diad axis. The third haem–polypeptide interaction is formed by the fifth position axial ligation of the ferric haem iron with $N^{\varepsilon 2}$ of His 122. The sixth ligand ferric iron coordination site is either unoccupied or ligated by a solvent molecule, consistent with the high-spin character of the haem iron[21,22]. Space-filling representations of the molecular structure show the haem environment to be highly asymmetric, with the imidazole side chain of the fifth haem iron ligand and two-thirds of the corresponding haem surface being exposed to the solvent. In contrast, the distal haem surface, which faces towards the dimer interface, is surrounded by aromatic or otherwise hydrophobic amino acid residues. Many of these packing interactions are provided by residues of the A helix, which are orientated so as to restrict access of exogenous ligands to the sixth haem iron coordination site through the most direct route to the molecular surface.

Because of the geometry of the monomer–monomer packing interaction, both haem groups of the molecule are situated on the same face of the dimer in nearly parallel orientation. Although this structural arrangement suggests that the haems of cytochrome *c′* may be situated so as to allow their simultaneous interaction with some physiological oxidoreductase, it is equally possible that this arrangement provides the basis for inter-haem communication in the molecule. Of relevance to the latter possibility is the fact that the 24 Å iron–iron vector is nearly coincident with the A–A′ inter-helix contact normal vector, which at 6.0 Å is the shortest inter-helical interaction in the entire molecule. As described above, it is residues of the A helix which principally provide the packing interactions about the unliganded, distal haem surface. Thus, it seems possible that any local structural alterations accompanying haem ligation or oxidoreduction could be communicated between the haems due to the intimacy of the A–A′ helix packing interaction.

The principal similarity between the cytochromes *c′* and the mitochondrial cytochromes *c* is the common presence of a Cys-X-X-Cys-His sequence which provides the covalent attachment points and fifth axial ligand for the haem prosthetic group. Otherwise, the molecules are distinctly different with respect to overall chain folding, sequential location of the haem-binding peptide, spin state and extent of haem exposure to the solvent. Similarly, almost the only major feature shared by the cytochromes *c′* and the globins is their high-spin haem character, the general nature of the haem environments being otherwise quite different in the two molecules. Nevertheless, the fact that the cytochromes *c′* and globins are both high-spin haem proteins which can bind exogenous ligands and occur in both monomeric and higher aggregate forms[2,6], suggests interesting parallels between these molecules which require further investigation.

This work and facilities were supported by NIH grants GM18528-11 to M.D.K., RCDAK04EY0013 to M.A.C., GM20102, RR00757, to N.H.X., and GM21534, GM25664 to F.R.S. and NSF grants GB36019X to M.D.K., PCM7804349 to M.A.C. and PCM7722495 to N.H.X. Structure determination was done in partial fulfilment of the requirements for a PhD at the University of Arizona by P.C.W. who was a Carl S. Marvel Fellow. F.R.S. received a Dreyfus Teacher-Scholar Award and the University of Arizona Computer Center also provided support.

Received 6 February; accepted 25 April 1980.

1. Vernon, L. P. & Kamen, M. D. *J. biol. Chem.* **211,** 643–675 (1954).
2. Bartsch, R. G. in *The Photosynthetic Bacteria* (eds Clayton, R. K. & Sistrom, W. R.) 249–279 (Plenum, New York, 1978).
3. Barrett, J. & Kamen, M. D. *Biochim. biophys. Acta* **50,** 573–575 (1961).
4. Salemme, F. R. *A. Rev. Biochem.* **46,** 299–329 (1977).
5. Taniguchi, S. & Kamen, M. D. *Biochim. biophys. Acta* **74,** 438–455 (1963).
6. Perutz, M. F. *A. Rev. Biochem.* **48,** 327–386 (1979).
7. Bloomer, A. C., Champness, J. N., Bricogne, G., Staden, R. & Klug, A. *Nature* **276,** 362–368 (1978).
8. Stubbs, G., Warren, S. & Holmes, K. *Nature* **267,** 216–221 (1977).
9. Stenkamp, R. E., Sieker, L. C., Jensen, L. H. & McQueen, J. E. Jr *Biochemistry* **17,** 2499–2504 (1978).
10. Ward, K. B., Hendrickson, W. A. & Klippenstein, G. L. *Nature* **257,** 818–821 (1975).
11. Hendrickson, W. A., Klippenstein, G. L. & Ward, K. B. *Proc. natn. Acad. Sci. U.S.A.* **72,** 2160–2164 (1975).
12. Banyard, S. H., Stammers, D. K. & Harrison, P. M. *Nature* **271,** 282–284 (1978).
13. Mathews, F. S., Bethge, P. H. & Czerwinski, E. W. *J. biol. Chem.* **254,** 1699–1706 (1979).
14. Weber, P. & Salemme, F. R. *J. molec. Biol.* **117,** 815–820 (1977).
15. Cork, C., Hamlin, R. C., Vernon, W., Xuong, Ng. H. & Perez-Mendez, V. *Acta crystallogr.* **A31,** 702–703 (1975).
16. Xuong, Ng. H., Freer, S. T., Hamlin, R., Neilson, C. & Vernon, W. *Acta crystallogr.* **A34,** 289–296 (1978).
17. Matthews, B. W. *Acta crystallogr.* **20,** 82–86 (1966).
18. Ambler, R. P. in *Abstr. 3rd int. Symp. Photosynthetic Prokaryotes* (ed. J. M. Nichols) E17 (Oxford, 1979).
19. Salemme, F. R. & Fehr, D. G. *J. molec. Biol.* **70,** 697–700 (1972).
20. Cusanovich, M. A. *Biochim. biophys. Acta* **236,** 238–241 (1971).
21. Ehrenberg, A. & Kamen, M. D. *Biochim. biophys. Acta* **102,** 333–340 (1965).
22. Maltempo, M. M., Moss, T. H. & Cusanovich, M. A. *Biochim. biophys. Acta* **342,** 290–305 (1974).

Molecular dynamics of ferrocytochrome *c*

Scott H. Northrup, Michael R. Pear & J. Andrew McCammon*

Department of Chemistry, University of Houston, Houston, Texas 77004

Martin Karplus

Department of Chemistry, Harvard University, Cambridge, Massachusetts 02138

The cytochromes *c* function as single-electron carriers in the mitochondrial electron transport chain[1,2]. The native structures of the proteins from different species are quite similar[1,2], as are the structures of the reduced and oxidized forms[3,4]. The 103-residue polypeptide chain of tuna cytochrome *c* contains 5 α-helical segments (residues 2–13, 50–54, 61–69, 71–74, 89–100); the haem group is almost completely buried in a hydrophobic pocket and is covalently bonded to the polypeptide chain by thioether linkages involving Cys 14 and Cys 17 and by linkages to the iron involving His 18 and Met 80 (refs 1–3). NMR[5,6] and hydrogen exchange[7,8] studies indicate significant internal mobility in cytochrome *c*. In spite of the apparent similarity of the time-average structures of the reduced and oxidized proteins, the structural fluctuations are significantly larger in the latter form[2,7,8]. It has been suggested that the internal motions have a role in the electron transfer mechanism[2,9]. A 16-ps computer simulation[10–14] of the atomic motions in reduced tuna cytochrome *c* has now been completed; this reveals various correlations between the magnitudes of the atomic position fluctuations and the structural features of the protein.

The dynamical simulation method used here is similar to that used in earlier studies of the pancreatic trypsin inhibitor[10]. The protein potential energy function consists of a sum of terms associated with bonds, bond angles, dihedral angles, hydrogen bonds and nonbonded (van der Waals and electrostatic) interactions. The partial charges of the atoms have been reduced according to the distances of the atoms from the protein centre to approximate dielectric screening effects due to surrounding water[15]. To begin the simulation, the protein was dynamically equilibrated as follows. The X-ray structure[16,17] was first subjected to 100 cycles of steepest descent energy minimization[18] to relax any sizeable local stresses. The atoms were then assigned random maxwellian

*To whom reprint requests should be addressed.

0028 0836/80/290304–02$01.00